JOURNAL OF MATERIALS SCIENCE 26 (1991) 5502–5508

Structural changes during mechanical alloying of elemental aluminium and molybdenum powders

M. V. ZDUJIC*, K. F. KOBAYASHI‡, P. H. SHINGU
Department of Metal Science and Technology, Kyoto University, Sakyo-ku, Kyoto 606, Japan

Mechanical alloying of elemental aluminium and molybdenum powders was performed by conventional low-energy ball milling. Seven compositions (Al–3, 10, 17, 20, 27, 50 and 75 at% Mo), as well as elemental aluminium and molybdenum powders, were milled up to 1000 h. The structural changes during milling were followed by X-ray diffraction. In all cases milling produced refinement of the microstructure, and prepared powders were microcrystalline with grain sizes of the order of nanometres. A supersaturated solid solution of molybdenum in aluminium was formed. Only for the Al–75 at% Mo powders was a solution of aluminium in molybdenum observed.

1. Introduction

Mechanical alloying is a powder metallurgy technique for the production of composite metal powders. It utilizes various types of milling machines in which a blend of different powders (elemental, prealloyed, intermetallic etc.) is subjected to highly energetic compressive forces. By repeated fracture and cold welding of the constituent powder particles, it is possible to make alloys from normally immiscible components. Mechanical alloying was first developed for the production of complex oxide dispersion-strengthened alloys [1]. The discovery that amorphous alloys can be prepared by mechanical alloying starting from crystalline powders [2] has promoted this previously neglected technique in one of the most attractive metal-processing route available today. Several reviews on mechanical alloying have appeared recently [3–5]. Alloying by melting of metals with significantly different melting points may present considerable problems, which may be overcome by mechanical alloying, as it is a solid-state process.

Aluminium–molybdenum, like other aluminium–transition metal systems, is a good candidate for processing by mechanical alloying. In this paper we present results of structural changes during mechanical alloying of elemental aluminium and molybdenum powders. Conventional low-energy ball milling was chosen, to enable us to perceive all the steps of mechanical alloying, as well to retain non-equilibrium structures that may appear in the resultant powders.

2. Experimental procedure

Elemental powders of aluminium (nominal purity 99.99% and particle size less than 150 μm (− 100 Mesh)) and molybdenum (nominal purity 99.98% and particle size 3 μm) were used as starting materials. Powders were weighted to obtain the desired proportion of starting powders.

Seven compositions were taken for investigation, namely Al–3, 10, 17, 20, 27, 50 and 75 at % Mo. Additionally, for comparison, elemental aluminium and molybdenum powders were milled separately under the same milling conditions as powder mixtures. The compositions were chosen by considering an Al–Mo phase diagram [6]. Mechanical alloying was carried out in a conventional horizontal ball mill. A cylindrical stainless-steel vial of inner diameter 130 mm and height 128 mm filled with stainless-steel balls of diameter 9.4 mm was used as milling tool. The vial was rotated at angular velocity 9.4 rad sec^{-1} (90 r.p.m.). The total weight of the balls was 4000 g, and the ball:powder-weight ratio was 90:1. The vial was loaded and sealed in a glove box in an argon atmosphere. Prior to milling 2.7 mass % methanol, as a process control agent, was added to the powder mixtures. To follow the process of mechanical alloying, milling was interrupted periodically and a small amount of powder was removed, also in a glove box, for analysis.

The microstructure of mechanically alloyed powders were observed by scanning electron microscopy (SEM) under a Hitachi X-650 microscope. The samples were prepared using standard metallographic techniques. A few compositions, namely Al–17, 20 and 27 at % Mo were observed after mechanical alloying by transmission electron microscopy (TEM) on the JEOL JEM-200CX equipment.

X-ray diffraction (XRD) analyses were performed on a Rigaku RAD-B diffractometer with CuK_α ($\alpha = 0.154$ nm) radiation, operating at 40 kV and

* On leave from Institute of Technical Sciences of Serbian Academy of Sciences and Arts, Belgrade, Yugoslavia.
‡ *Present address*: Department of Welding and Production Engineering, Osaka University, Suita, Osaka, 565 Japan.

0022–2461/91 $03.00 + .12

20 mA. Scan speed was 0.02 deg s^{-1}. All X-ray data were stored on a computer for further analysis. Peak intensities were corrected for background, polarization, $K\alpha_{1,2}$ separation as well as for instrumental broadening.

In order to determine the composition of the powders after mechanical alloying, chemical analysis was done on a few powders, namely Al–17, 27 and 27 at % Mo after milling for 1000 h. Chemical analysis was done by the inductive coupled plasma (ICP) technique; the results are given in Table I.

3. Results and discussion

The microstructural evolution of the powders subjected to mechanical alloying is presented in Fig. 1. The starting blend of the elemental powders consisted of fine agglomerated molybdenum particles and much larger well-shaped aluminium particles (milling time 0 h). As a result of intensive cold welding and fracture of the constituent aluminium and molybdenum powder particles, composite particles had already formed after 30 h of milling. More brittle molybdenum was embedded in the aluminium matrix. Further milling refined the microstructure, and after 100 h of milling the molybdenum was finely dispersed in the aluminium matrix. Particle size increased due to intensive cold welding. After 300 h of milling, a uniform single-phase microstructure was formed: molybdenum dispersoids could not be resolved by SEM. Also, a decrease in particle size is obvious, indicating that at this stage particle fracture prevailed over cold welding. Prolonged milling time further decreased particle size (milling time 1000 h) and particles became more rounded in shape. No significant change could be resolved by SEM in a comparison of the microstructures of mechanically alloyed powders milled for 300 and 1000 h.

The XRD patterns of the mechanically alloyed powders of two characteristic compositions for various milling times are presented in Fig. 2. As milling

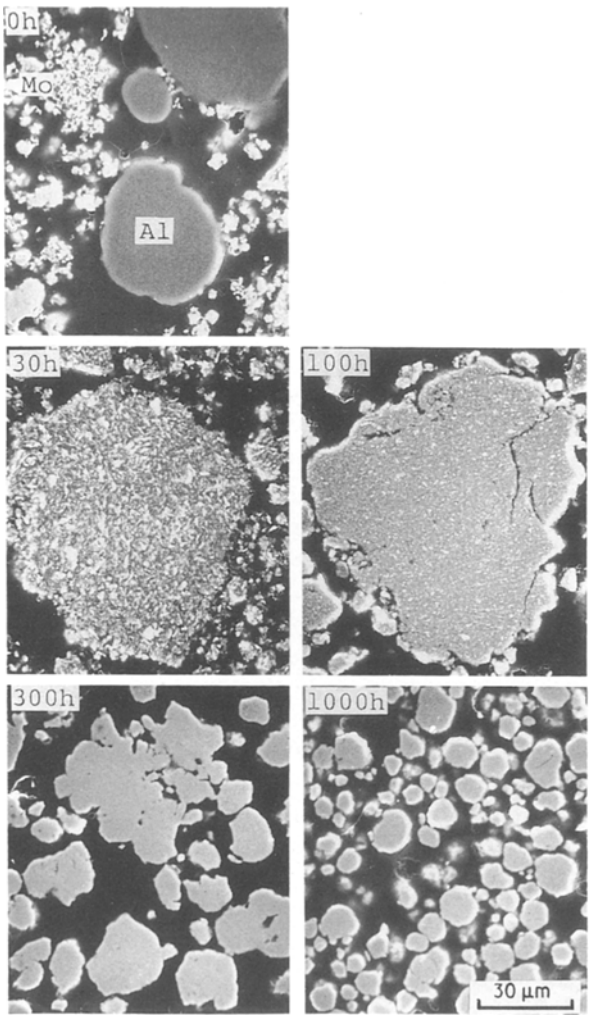

Figure 1 SEM micrographs of the mechanically alloyed Al–27 at % Mo powders after various milling times.

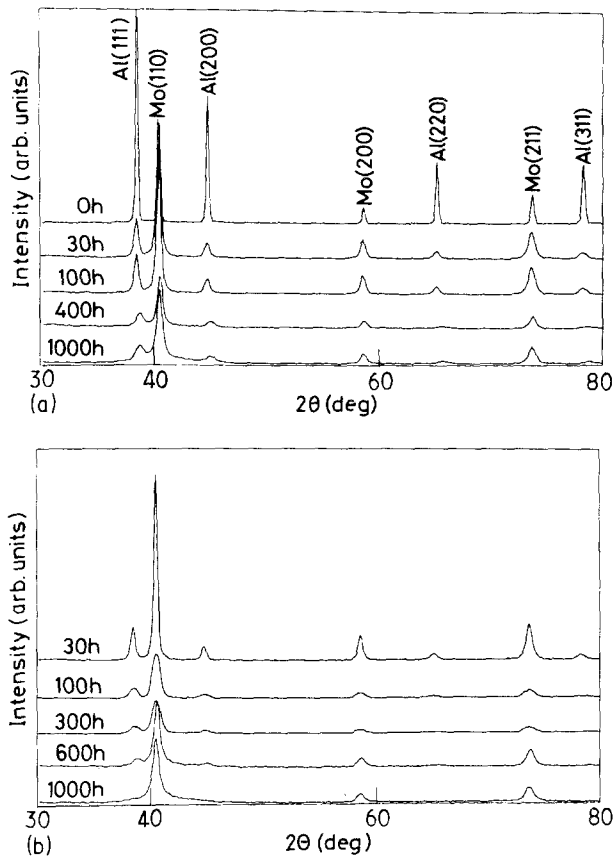

Figure 2 XRD patterns of the mechanically alloyed Al–17 at % Mo (a) and Al–20 at % Mo (b) powders after various milling times.

TABLE I Chemical composition of the mechanically alloyed Al–17, 27 and 50 at % Mo powders milled for 1000 h

Nominal composition	Al (at %)	Mo (at %)	Fe (at %)	Ni (at %)	Cr (at %)
Al–17 at % Mo	83.494	16.342	0.146	0.005	0.012
Al–27 at % Mo	72.494	26.540	0.859	0.044	0.064
Al–50 at % Mo	52.489	46.602	0.796	0.036	0.079

time increased, both the aluminium and molybdenum peaks broadened and the intensity of aluminium peaks decreased. The aluminium peaks shifted to higher angles. For example, for the Al–17 at % Mo mixture before milling, the aluminium line was at $2\Theta = 38.45°$, and shifted to $2\Theta = 38.62°$ for the powders milled for 1000 h. The position of the molybdenum peaks remained almost constant for all milling times. As can be seen from Fig. 2, in the mechanically alloyed Al–17 at % Mo powders both aluminium and molybdenum peaks are still visible even in the final powders milled for 1000 h, whereas for the Al–20 at % Mo powders, aluminium peak intensities continuously decrease as milling time increases and disappear completely for the sample milled for 1000 h.

The XRD patterns of aluminium–molybdenum mechanically alloyed powders as a function of composition are presented in Fig. 3. Up to 17 at % Mo, both the aluminium and molybdenum peaks are visible in the diffraction patterns and for compositions with $\langle Mo \rangle = 20$ at % Mo, only molybdenum peaks can be resolved. Furthermore, it can be seen that molybdenum peaks are broader with the increase in molybdenum concentration.

To follow the refinement of a structure due to milling, the Scherrer formula [7] was used: $D = 0.9\lambda/\beta\cos\theta$ where D is the mean crystallite dimension normal to diffracting planes, λ is the X-ray wavelength ($\lambda = 0.15406$ nm), β is the peak width at half-maximum peak height (radians) and θ is the peak position.

The aluminium and molybdenum crystallite size as a function of milling time for the mechanically alloyed Al–17 at % Mo powders, as well as for the elemental aluminium and molybdenum powders milled separately, is presented in Fig. 4. The crystal grain size of both aluminium and molybdenum in the starting powders before milling was about 40 nm. The crystallite size decreased very rapidly at the start of milling in elemental powders, and also in all the mixtures investigated. It is obvious that milling produces the most effective crystallite size reduction in elemental molybdenum powders. After about 300 h, the crystallite size reached minimal value, and for elemental molybdenum powders it was about 5 nm. These values remained almost constant for further milling times. In the mechanically alloyed Al–17 at % Mo powders, minimal values of crystallite size were about 13 and 16 nm for aluminium and molybdenum, respectively. For the elemental aluminium powders, the trend seems somewhat different. After reaching minimal values of about 20 nm for the milling time of about 100 h, the crystallite size slightly increased to values of about 26 nm for further milling time. We explain this phenomenon as follows. As aluminium is very ductile, after a long milling time the methanol (added as a process control agent) could not prevent cold welding. Between milling times of 650 and 1000 h, all the aluminium powder was cold welded to balls and vial walls, and examination of the powder milled for 1000 h was not possible.

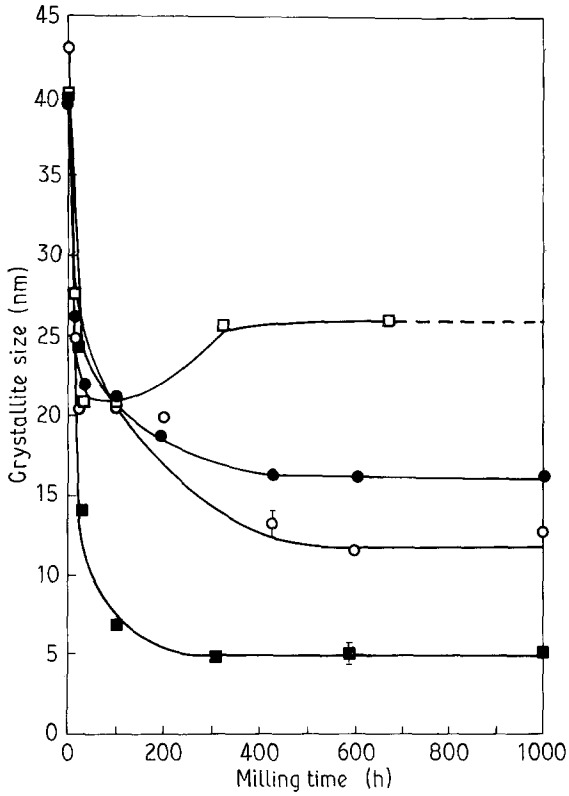

Figure 4 Crystallite size of aluminium and molybdenum calculated by the Scherrer formula from the Al(1 1 0) line and Mo(1 1 1) line as a function of milling time. □, Al elemental; ■, Mo elemental; ○, Al (Al–17 at % Mo); ●, Mo (Al–17 at % Mo).

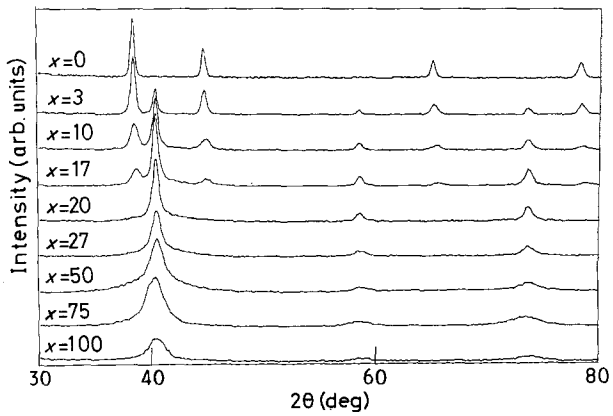

Figure 3 XRD patterns of mechanically alloyed powders as a function of molybdenum content. Milling time for all compositions was 1000 h except for elemental aluminium powders, milled for 650 h.

The dependence of the molybdenum crystallite size on molybdenum content is presented in Fig. 5. Obviously, as the molybdenum content increases, reduction of the crystallite size is more effective. For example, in the mechanically alloyed Al–3 at % Mo powders, molybdenum crystallite size was about 23 nm and decreased to about 5 nm for the Al–75 at % Mo powders. This indicates that aluminium acts as an inhibitor of molybdenum crystallite size reduction.

In comparison, crystallite size (effective particle size) in the mechanically alloyed amorphous $Ni_{60}Nb_{40}$ and Ni–Ge powders, also calculated by the Scherrer formula, is about 1–2 nm [2, 8].

From the XRD patterns, the most intensive lines of aluminium and molybdenum, namely Al(1 1 1) and

Mo(1 1 0), were used to calculate the lattice parameters. The change of aluminium and molybdenum lattice parameters as a function of milling time for the mechanically alloyed Al–3, 10 and 17 at % Mo (aluminium rich compositions) as well as for the elemental aluminium and molybdenum powders, is presented in Fig. 6. In the elemental aluminium and molybdenum powders milled separately, almost the same trend can be observed. As milling time increased, the lattice parameters of both aluminium and molybdenum increased to maximum values, and as milling continued they decreased. Such results indicate that uniform macrostrain was accumulated during milling. However, it seems that after some milling time, the powder becomes more relaxed in respect to uniform macrostrain.

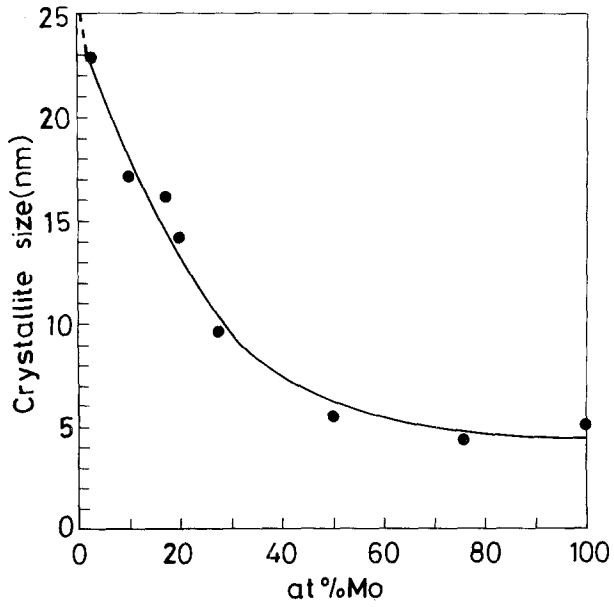

Figure 5 Molybdenum crystallite size as a function of molybdenum content. Milling time, 1000 h.

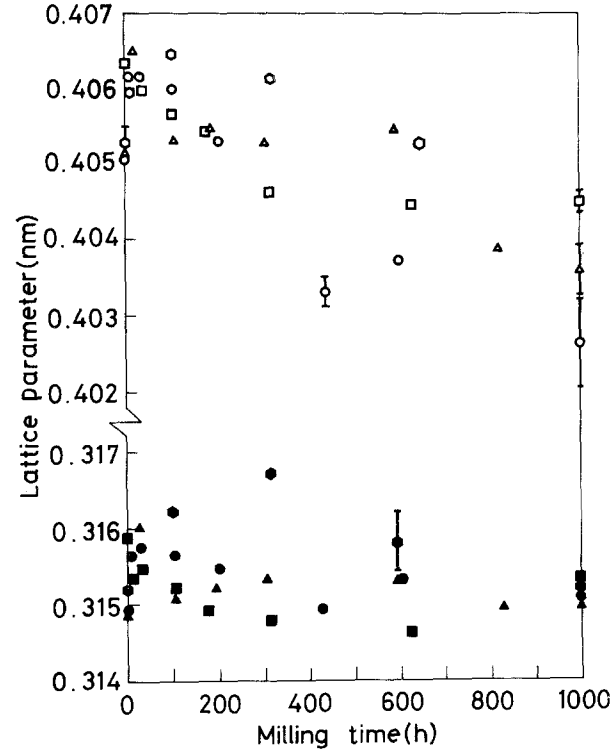

Figure 6 Lattice parameters of aluminium and molybdenum calculated from the Al(1 1 0) line and Mo(1 1 1) line as a function of milling time. ⬡, elemental; □, △, ○, Al–3, 10, and 17 at % Mo, respectively. Open symbols, Al; closed symbols, Mo.

In general, considering all the results obtained from the X-ray examination, it can be seen that during milling, due to plastic deformation, powders are subjected to crystallite size reduction and accumulation of both uniform macrostrain and non-uniform microstrain [9].

For the powder mixtures, different results were obtained. Lattice parameters of both aluminium and molybdenum increased at the very beginning of milling (initial stages less than about 100 h). As mechanical alloying progressed, refinement of the microstructure occurred. The aluminium lattice parameter decreased while the molybdenum lattice parameter remained almost constant (Fig. 6). The calculated value of the aluminium lattice parameter in the elemental aluminium powder is $0.4053 \pm 2.3 \times 10^{-4}$ nm, whereas for the mechanically alloyed Al–3, 10 and 17 at % Mo powders milled for 1000 h, it is $0.4046 \pm 0.9 \times 10^{-4}$, $0.4036 \pm 3.3 \times 10^{-4}$ and $0.4026 \pm 5.8 \times 10^{-4}$ nm, respectively. Such results indicate that a supersaturated solid solution of molybdenum in aluminium was formed.

The amount of molybdenum in solid solution increased as milling time increased (Fig. 6). From a linear extrapolation of the rapidly quenched Al–Mo alloy data [10], the amount of molybdenum entrapped in supersaturated solid solution obtained by mechanical alloying can be roughly estimated. Thus about 0.4, 1.3 and 2.4 at % molybdenum was in solution in aluminium for the mechanically alloyed Al–3, 10 and 17 at % Mo powders milled for 1000 h. The equilibrium solid solubility of molybdenum in aluminium is less than about 0.07 at % [6].

The molybdenum lattice parameter in the mechanically alloyed Al–20, 27, 50 and 75 at % Mo powders (molybdenum rich compositions) as a function of milling time is presented in Fig. 7. As already stated

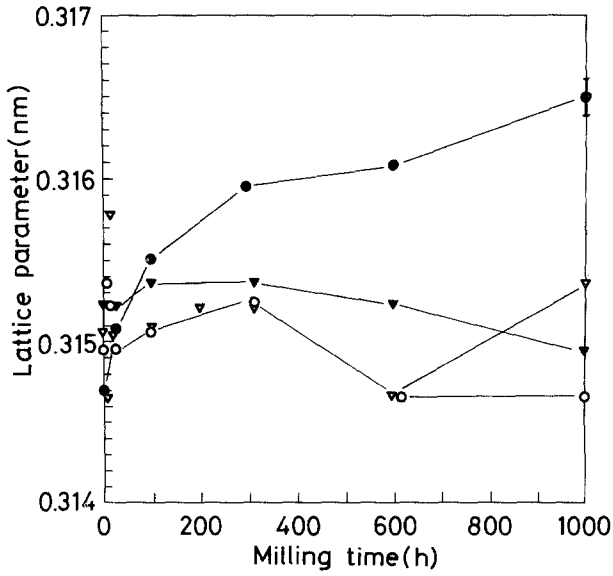

Figure 7 Lattice parameters of molybdenum calculated from the Mo(1 1 1) line as a function of milling time. Al–▽, 20; ▼, 27; ○, 50; ●, 75 at % Mo.

for these compositions, XRD patterns of the final products show only molybdenum peaks (Fig. 3). In the Al–20, 27 and 50 at % Mo powders (Fig. 7) the molybdenum lattice parameter does not change significantly, and shows almost the same trend as a function of milling time. The exception is the Al–75 at % Mo composition. For these samples, the molybdenum lattice parameter continuously increased as milling time increased, indicating that a solid solution of aluminium in molybdenum was obtained.

In order to back up the results of grain-size estimation obtained from X-ray measurements, TEM was employed for observation of a few powders after mechanical alloying was completed. Relevant TEM micrographs of the mechanically alloyed Al–17, 20 and 27 at % Mo powders milled for 1000 h are presented in Figs 8 and 9. For all samples, bright- and dark-field images correspond to the centre and first (diffuse) ring on the associated electron diffraction pattern, respectively.

TEM micrographs reveal a very fine microcrystalline structure with the grain (crystallite) sizes in the range from 5 to 50 nm. It can be recognized that grain size becomes smaller as molybdenum content increases (compare micrographs of Al–17, 20 and 27 at % Mo powders). Crystalline material is embedded in a matrix which appears to be very disordered (a supersaturated solid solution of molybdenum in aluminium) and which appears to be amorphous. The electron diffraction pattern shows one diffuse ring which corresponds to a disordered or amorphous phase, and a series of sharp rings. For the Al–17 at % Mo samples, diffraction rings are from both aluminium and molybdenum, whereas for the Al–20 at % Mo samples, only rings from molybdenum are revealed (Fig. 8). In Fig. 9, TEM micrographs of the mechanically alloyed Al–27 at % Mo powders, as-milled as well as heat-treated up to 973 K, are presented. Powders were heated in differential scanning calorimetry (DSC) as well as in differential thermal analysis (DTA) cells, and almost the same results were obtained. Exothermic peaks with maximum at about 770 K appeared in both DSC and DTA curves.

It can be seen that further disordering of the material occurred due to heat treatment. The material appears to be a mixture of crystalline and amorphous

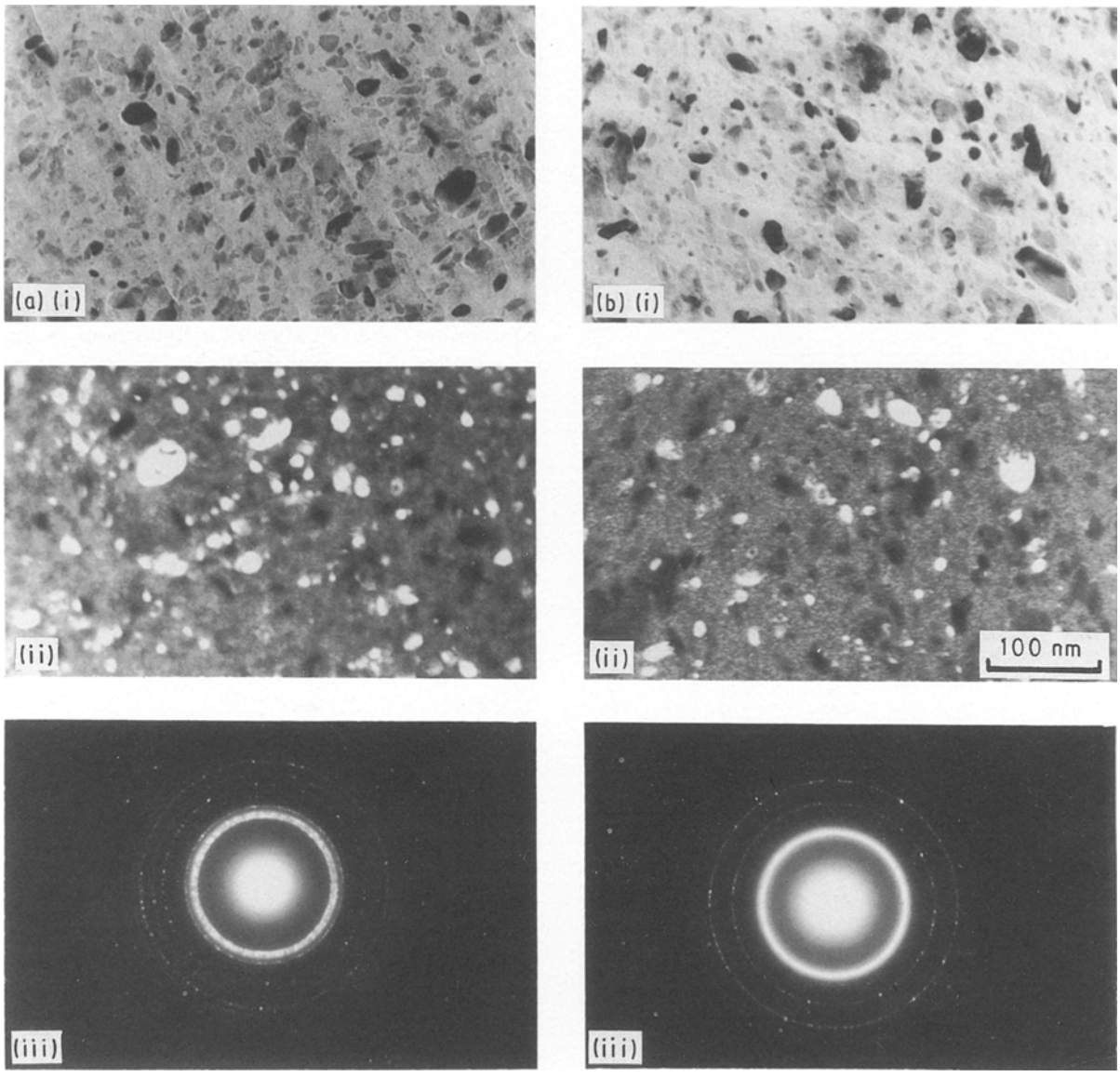

Figure 8 TEM micrographs (i) bright-field and (ii) dark-field, and (iii) associated electron diffraction patterns of mechanically alloyed (a) Al–17 at % Mo and (b) Al–20 at % Mo powders.

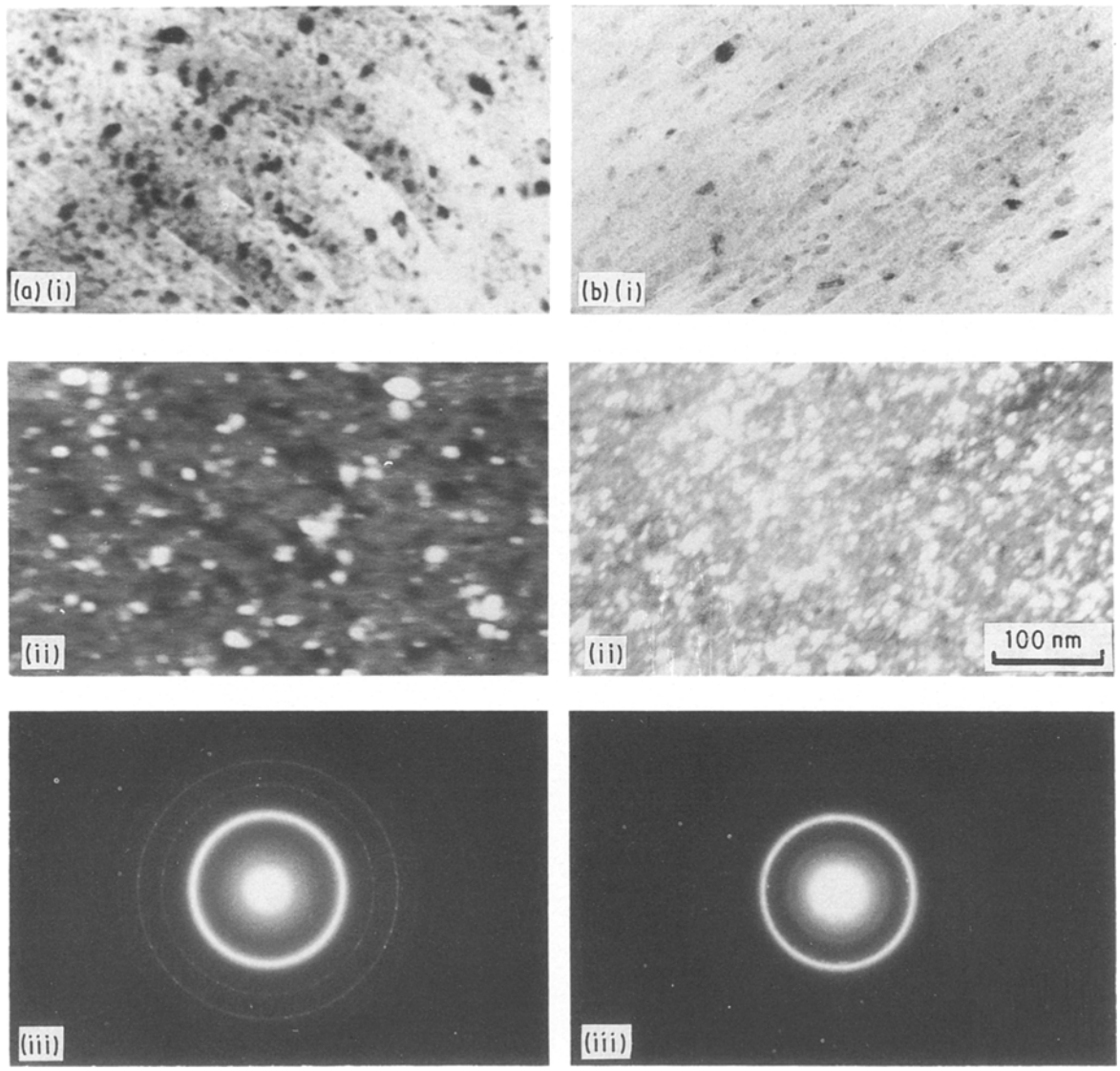

Figure 9 TEM micrographs (i) bright-field and (ii) dark-field, and (iii) associated electron diffraction patterns of the mechanically alloyed Al–27 at % Mo powders (a) as-milled and (b) after heat treatment in a DTA cell in argon atmosphere (continuous heating up to 973 K, heating rate 0.33 K s^{-1}).

structures. The electron diffraction pattern of the heat-treated sample shows only one diffuse ring (compare Fig. 9 bottom left and right). Several spots from the molybdenum crystal grains can also be detected. This disordering phenomenon was also confirmed by the XRD analysis as shown in Fig. 10. Comparing the X-ray patterns of the as-milled powders and those heat-treated up to 973 K, it can be seen that the principal peak is shifted to lower angles, and new very weak peaks appear in the heat-treated sample. This suggests that an intermetallic compound with very fine grain size was already formed at these relatively low temperatures. However, it appears that this intermetallic compound may have a very deformed crystal structure.

Heat treatment of the powders to higher temperatures resulted in the formation of the stable intermetallic compound Al_8Mo_3. In Fig. 10, the XRD patterns are presented of the mechanically alloyed Al–27 at % Mo powders milled for 1000 h and heat treated continuously (heating rate 0.33 K sec^{-1}) in a DTA cell in argon atmosphere up to various final temperatures. Inspection of the line positions revealed that the intermetallic compound Al_8Mo_3 was formed.

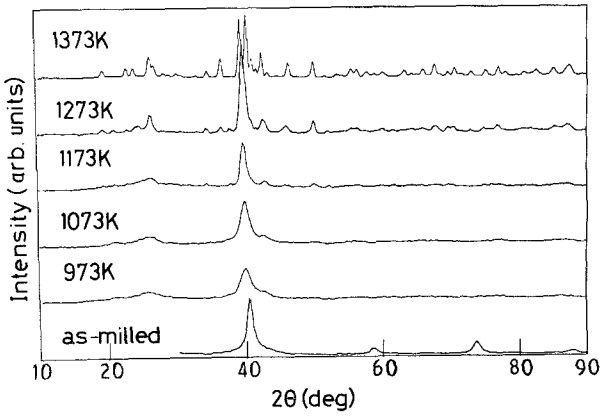

Figure 10 XRD patterns of the mechanically alloyed Al–27 at % Mo powders milled for 1000 h and after continuous heat treatment to different final temperatures in a DTA cell in argon atmosphere (heating rate 0.33 K s^{-1}).

4. Conclusions

Mechanical alloying by conventional low-energy ball milling of elemental aluminium and molybdenum powders in the wide composition range from 3 to 75 at % Mo was studied. The main conclusions are as follows.

1. Mechanical alloying produces very fine composite powders with a microcrystalline structure. The crystallite sizes are of the order of nanometres.

2. Very fine molybdenum dispersoids are embedded in a disordered supersaturated aluminium matrix.

3. The amount of molybdenum entrapped in supersaturated solution increases as the molybdenum content in the powders increases.

4. A solution of aluminium in molybdenum is only observed for the composition Al–75 at % Mo.

5. The effect of milling on the reduction of molybdenum crystallite size depends on aluminium content. Molybdenum crystallite size becomes smaller as aluminium content decreases.

6. By the heat treatment at relatively low temperatures (993 K) of as-milled powders, the structure of the Al–27 at % Mo samples becomes more disordered and appears to be amorphous.

Acknowledgements

The authors thank J. Kuyama and N. Inoue for preparation and observation of the samples by TEM, and K. Ishihara for helpful discussions.

References

1. J. S. BENJAMIN, *Met. Trans.* **1** (1970) 2943.
2. C. C. KOCH, O. B. CAVIN, C. G. McKAMEY and J. O. SCARBROUGH, *Appl. Phys. Lett.* **43** (1983) 1017.
3. R. SUNDARESAN and F. H. FROES, *J. Met.* **39** (1987) 22.
4. A. W. WEEBER and H. BAKKER, *Physica B* **153** (1988) 93.
5. C. C. KOCH, *Ann. Rev. Mater. Sci.* **19** (1989) 121.
6. T. B. MASSALSKI (ed.) in "Binary Alloy Phase Diagrams", Vol. 1 (American Society for Metals, Metals Park, Ohio, 1986) p. 133.
7. S. F. BARTRAM, in "Handbook of X-rays", edited by E. F. Kaeble (McGraw-Hill, New York, 1967) p. 17-1.
8. C. POLITIS, *Physica B* **135** (1985) 286.
9. B. CULLITY, "Elements of X-ray Diffraction", 2nd edn. (Addison-Wesley, Reading, Massachusetts, 1978) p. 447.
10. N. I. VARICH, L. M. BUROV, K. Ye. KOLESNICHENKO and A. P. MAKSIMENKO, *Fiz. metal. metalloved.* **15** (1963) 292.

Received 2 April
and accepted 20 December 1990